Recombination photophysics in AgCl

1990 J. Phys.: Condens. Matter 2 3021

(http://iopscience.iop.org/0953-8984/2/13/011)

J. Phys.: Condens. Matter 2 (1990) 3021–3030. Printed in the UK

Recombination photophysics in AgCl

J P Spoonhower, F J Ahlers, R S Eachus and W G McDugle
Corporate Research Laboratories, Eastman Kodak Company, Rochester, NY, USA

Received 24 October 1989

Abstract. ODMR investigations of recombination processes in AgCl have been extended in an effort to reconcile the apparently contradictory interpretations of other workers. The experiments described here indicate that for AgCl no single recombination mechanism dominates for low-temperature excitations; the energy can relax either by a donor–acceptor pair recombination, or by an excitonic recombination. Background impurity levels could determine the relative intensities of ODMR transitions associated with these two recombination processes. Only shallowly trapped (isotropic) electrons have been identified from analysis of these spectra; no tetragonally distorted electron traps have been observed. By way of contrast, only deeply self-trapped holes (STH) are seen. Yamaga's models for the two self-trapped excitons (STE) are shown to describe adequately the ODMR data for all transitions associated with the excitons in AgCl. Observation of the STE by EPR is shown to be possible because of the excessive excited-state lifetime of this species.

1. Introduction

Controversy over the exact nature of the recombination processes that control the low-temperature photophysics of silver chloride exists because of a lack of agreement over the assignment of certain ODMR spectral features observed by a number of workers. Marchetti and co-workers identified the resonances due to the self-trapped hole (STH) and a nearly free electron (Marchetti *et al* (1978) and Marchetti and Tinti (1981)). These assignments were based upon comparison with g-values from EPR data (Eachus *et al* 1978), and in the case of the self-trapped hole, chlorine hyperfine splitting in the $g_\perp$-region (Höhne and Stasiw 1968). A set of three lines in the centre portion of the spectrum was assigned to an electron trap with tetragonal symmetry; this centre was not unambiguously identified. At 4.2 K, the signals characteristic of the self-trapped exciton (STE) were largely, if not entirely, missing, under the conditions of these experiments. Subsequent work by Marchetti and co-workers examined the ODMR in AgBr and AgBrI, where a donor–acceptor recombination mechanism was shown to dominate the recombination photophyics (Marchetti and Burberry 1983, 1985, Burberry and Marchetti 1985). Recently, it has been suggested that an intermediate-case exciton (near-neighbour donor–acceptor pair) may play a role in the luminescence of AgBr (Marchetti *et al* 1988).

Hayes and Owen (1978), and then Yamaga and co-workers (Yamaga and Hayes 1982a, b, Yamaga *et al* 1983, Yoshioka and Yamaga 1985, Yoshioka *et al* 1985, Sugimoto *et al* 1985, Yamaga and Yoshioka 1987) identified and analysed the STE in their ODMR

0953-8984/90/133021 + 10 $03.50

spectra. Two species were seen: an intrinsic, or unassociated STE, and a bromine-associated STE. The bromine impurity is ubiquitous in AgCl. The former was shown to have tetragonal symmetry and to dominate the observed spectrum at 4.2 K, whereas for the latter, orthorhombic symmetry was proposed; this centre was most evident at lower temperatures. Very weak signals from the STH and the nearly free electron were seen. All the work cited above corrected the erroneous assignment of the Br^- STE spectral features to the intrinsic STE (Murayama *et al* 1976). In Yamaga's subsequent work it was proposed that Jahn–Teller effects play an important role in the dynamics of these defects (Yamaga *et al* 1985); the existence of these effects is required for a complete understanding of the ODMR spectra.

The resolution of these two viewpoints is the main focus of this report. We employ the model developed by Yamaga for the STE in the analysis of the ODMR data. Measurements of the wavelength dependence of ODMR in both emission and excitation are presented. The dependence of the ODMR intensities on the modulation frequency has been extended to the case of the ODMR lines of the bromine-associated STE.

2. Experimental

Powdered AgCl was prepared from doubly recrystallised $AgNO_3$ and excess HCl (Merck, 'Suprapure' grade) and washed with de-ionised water until the wash solutions were free of chloride ions and neutral in pH. This material was then dried in the dark at 80 °C for two weeks. Powdered AgCl was melted in a pyrolytic, graphite-coated, quartz tube under vacuum, and then gaseous chlorine (Matheson, Semiconductor grade) was bubbled through the molten AgCl for six hours. Single crystals of AgCl were grown in the same quartz tube, under vacuum, by the Bridgman method; these were oriented by x-ray diffraction methods, and then cut and polished for mounting in the cryostats. Individual inadvertent contaminants were <4 molar ppm, as determined by spark-source mass spectrometry or emission spectroscopy.

ODMR spectra were obtained using two different instruments. The apparatus used for 36 GHz spectra has been described in detail previously (Marchetti and Tinti 1981). Both field and amplitude modulation methods are provided for on this instrument. Approximately 1.0 W of microwave power was available. The Voigt geometry was routinely employed for ODMR at 36 GHz and for level anti-crossing (LAC) measurements using magnetic field modulation.

At 24 GHz, a custom Oxford Instruments SM4 cryomagnet was employed to obtain both ODMR and LAC spectra. For ODMR, only amplitude modulation was available. Typical modulation frequencies ranged from 10 to 600 Hz. The maximum available microwave power from the klystron oscillator was 600 mW. The Faraday geometry was used for these ODMR experiments. For LAC spectra, the signal was measured as the difference between right and left circularly polarised light in the Faraday configuration; a quartz modulator produced the polarisation modulation.

Emission spectral dependences of the signals were measured using a 0.85 m double monochromator with a bandpass of approximately 50 cm^{-1}; the excitation spectral dependence was measured using a 0.25 m monochromator and a xenon lamp. The spectral bandpass in excitation was quite large, of the order of 10 nm. The excitation spectra were corrected for intensity variation of the lamp and monochromator by the use of a Rhodamine B quantum counter solution.

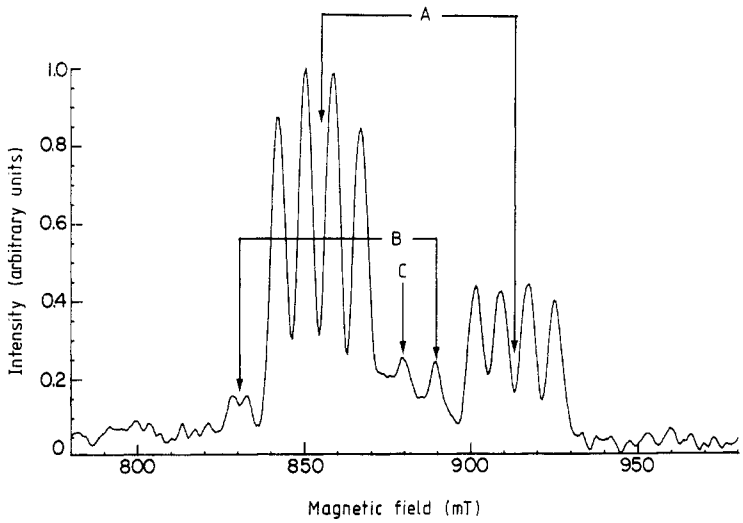

Figure 1. ODMR signal intensity versus magnetic field. T = 1.6 K. Excitation wavelength = 365 nm, emission wavelength = 490 nm, modulation frequency = 325 Hz, microwave frequency = 24.092 GHz.

EPR measurements were made on a Varian E-12 spectrometer with an E-110 35 GHz microwave bridge and E-265 liquid helium cryogenic accessories. The TE_{011} cylindrical cavity was modified to allow light access with a 1 mm diameter hole in the side wall. A 200 W, high-pressure Hg lamp, monochromator, and 365-line filter provided bandgap illumination. EPR measurements at 1.8 K were made using a conventional immersion helium cryostat with provision for pumping on the cryogen reservoir.

3. Results and discussion

ODMR spectra for a AgCl crystal with the magnetic field oriented along [100] are displayed in figures 1 and 2. Note that different temperature and wavelength specifications produce the rather different looking spectra that appear in these figures. The conditions chosen to produce these spectra are optimum for the bromine STE (lines A in figure 1) and the bare STE (figure 2). Also note in figure 2 the appearance of lines assigned to the STH and the nearly free electron. These lines appear at 810, 850, and 927 mT, respectively.

Lines B and C in figure 1 have been asigned to the two perpendicular configurations of the bromine STE, that is, to configurations where the y and z defect axes are oriented along the magnetic field direction (Yamaga and Hayes 1982a, b). Refer to figure 3 for a schematic representation of this defect.

There are two distortions that reduce the symmetry of the defect from octahedral to orthorhombic. Substitution of Br^- for Cl^- produces a tetragonal distortion; in addition, a Jahn–Teller distortion of the complex is believed to occur in the plane perpendicular to the Ag^+–Br^- axis. These two distortions are quantified in the spectroscopic values D and E for the exciton. It is interesting to note that $D \simeq 3E$ (Yamaga and Hayes 1982b). Because of this, the fine-structure splittings for the lines A and B are identical; that for the 'C' configuration is zero.

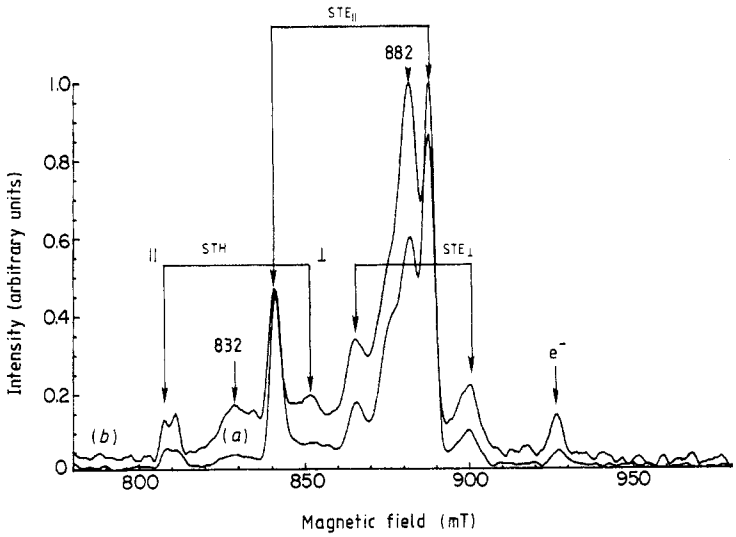

Figure 2. ODMR signal intensity versus magnetic field. $T = 4.2$ K. Excitation wavelength = 313 nm, emission wavelength = 510 nm, modulation frequency = 102 Hz (lower curve) and 325 Hz (upper curve), microwave frequency = 24.265 GHz.

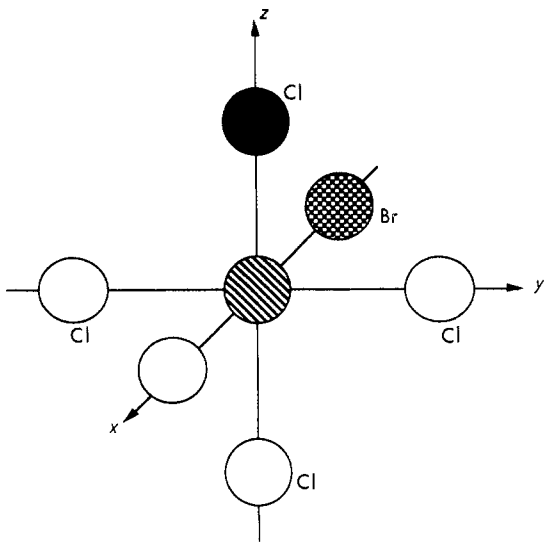

Figure 3. Schematic representation of the Br^- STE. The central silver ion is surrounded by six halogen ions. Chloride ions are shown as white, whereas bromide is shown as a crosshatched pattern. One of the chloride ions (black) undergoes a Jahn–Teller distortion.

The lines B and C in figure 1 appear at approximately the same field positions as some of the more prominent features that appear in figure 2; this is especially true for the central lines that appear in the spectrum obtained with 325 Hz modulation frequency. Wavelength dependences in both emission and excitation were used to test the assignment of the B and C lines to transitions of the Br^- STE. These data are shown in the figures that follow. Figure 4 shows uncorrected ODMR emission spectra for both the B (full) and C (broken) curves taken with a 0.85 m monochromator. The spectral contours are identical given the signal-to-noise ratio for this experiment. Both curves compare favourably with the emission spectral dependence of the LAC signal (see below) obtained

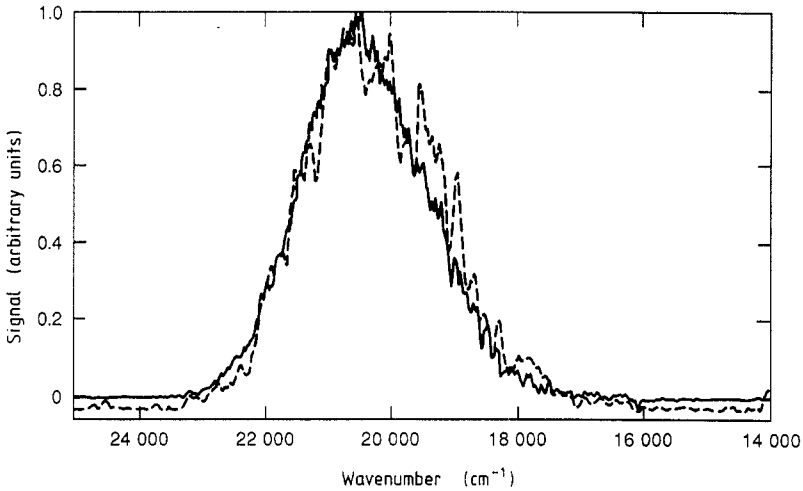

Figure 4. Emission wavelength dependence of ODMR transitions. Full curve: data for B; broken curve: data for C lines of figure 1.

at low magnetic fields under the same excitation and temperature conditions as figure 1 and with the total emission curve.

LAC spectra were measured under wavelength and modulation frequency conditions that should have optimised detecting such signals from the intrinsic STE and the Br^- STE. In the latter case a broad resonance with a maximum at approximately 29.4 mT was seen. None of the details assigned to hyperfine transitions (Marchetti and Tinti 1981) were observed; presumably, slight misalignment of the crystal and the lower Br^- level in our unintentionally doped crystal accounts for this difference. Quite possibly, this difference may also be related to the fact that intensity changes were detected in the earlier experiments, whereas polarisation changes are reported here. The wavelength dependence of this signal was well matched with the spectral dependence of the high-field doublet of quartets assigned to the Br^- STE. Under conditions that optimise the detection of the high-field resonances from the intrinsic defects, no additional LAC signal was observed. This is in contradistinction to earlier results (Marchetti and Tinti 1981). We did detect a weakened version of the LAC signal that arises from the Br^- STE; it was impossible to eliminate this signal completely in our experiments. Recall that in the experiments reported here the LAC signal is detected as the difference in circularly polarised light components. Any mechanism that reduces this polarisation difference could account for the observation of a much-weakened LAC signal. Our observation is consistent with either predominantly donor–acceptor-type recombination, or with an exciton recombination that obeys different polarisation selection rules.

Figure 5 shows corrected excitation spectra for one of the low-field components in the doublet of quartets marked A (full circles), and the two components of the doublet B. The low-field component of B is marked with triangles; the high-field component is marked with squares. We did not measure the excitation dependence of the C line because of the overlap with the A lines and its relatively small intensity. The excitation spectrum of the high-field component of the bare $STE_{\|}$ (line at approximately 887 mT in figure 2) is also shown in this figure for comparison. Based upon these measurements, we believe that the assignment of the B and C lines to a bromine-containing complex is

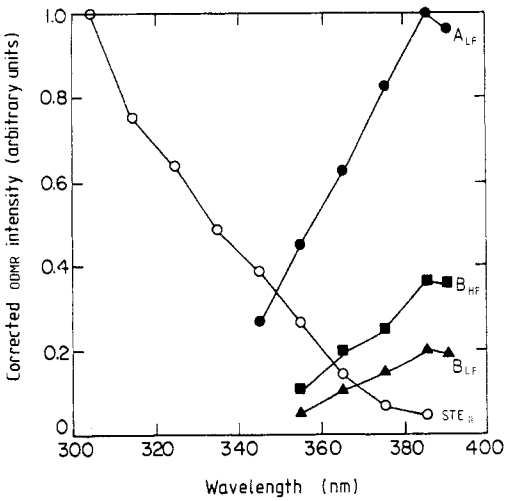

Figure 5. Excitation wavelength dependence of ODMR transitions. See text for an explanation of the data represented.

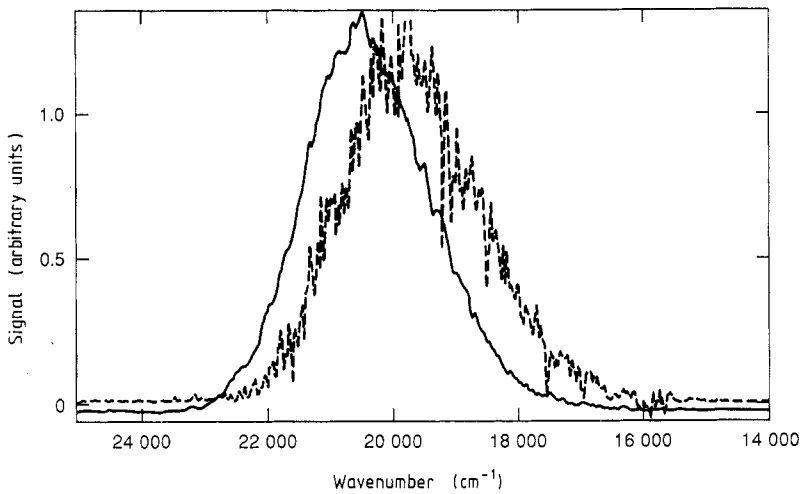

Figure 6. Emission wavelength dependence of ODMR transitions. Full data are for the low-field LAC signal; broken data are for the 887 mT ODMR line.

correct. Consistent with this assignment is the observation that *all* the lines displayed in figure 1 have the same dependence on the microwave modulation frequency; this dependence is markedly different for the transitions of the Br^- STE and the STE in AgCl. Our result for the modulation frequency dependence of the A lines is in agreement with the result of Yamaga; experimental results for the B and C lines were not available in this earlier work.

Figure 6 displays the emission spectrum for the high-field component of the $STE_{\|}$ with the spectrum of the LAC signal from the Br^- STE. There is a characteristic red-shift of the emission maximum for all of the ODMR transitions of the STE when the compared with the emission spectrum of the transitions of the Br^- STE. A similar shift of the emission wavelength maximum can be observed for the total emission under these same conditions.

The intense feature in the centre of the ODMR spectrum in figure 2 at 882 mT (g = 1.98) has the same spectral dependence as the STE features. However, its modulation frequency dependence is different from that of the STE lines in that it is enhanced for higher modulation frequencies (see figure 2(*b*)). This line is isotropic and has a g-value equal to the average of the g-values for the parallel and perpendicular configurations of the STE, that is

$$\bar{g} = (g_{\parallel} + 2g_{\perp})/3.$$

Our 24 GHz spectra, when compared with those of Yamaga, show better separation of the lines due to the STE and the Br^- STE, brought about by the judicious choice of optical wavelengths. This makes this central line more evident. The fact that the emission spectrum for this line matches that of the other STE lines (and the STH) strongly suggests that this transition does not originate from the bromide complex. The fact that the modulation frequency dependence for this line differs from that of the other STE lines is consistent with Yamaga's X-band results. Our 36 GHz ODMR experiments (see below) are also consistent with this observation.

In our spectra, an additional broad line at 832 mT appears between the STH parallel and perpendicular lines with the increase of the modulation frequency. Its intensity increase correlates with the intensity of the strong central feature (882 mT) assigned by Yamaga to the dynamic average of the STE lines (Yamaga *et al* 1985). Note that if one takes the average of this line's g-value (2.08) and nearly free electron's g-value (1.88),

$$g_{\text{avg}} = (g_{\text{unknown}} + g_{\text{e}})/2$$

the computed g_{avg} matches the intense isotropic line position to within experimental error. An additional weak shoulder can also be seen on the low-field side of the 882 mT resonance. Its intensity does not increase with increasing modulation frequency. We have not made an assignment to this line; its weakness and the overlap with the 882 mT line make determination of its wavelength dependence impossible.

The g-value for the unknown line at 832 mT is approximately correct for Cu^{2+} in AgCl if we assume that the impurities are not well dispersed (Burnham and Moser 1964). Features in the $g_{\parallel}$-region of the AgCl:Cu^{2+} EPR spectrum are difficult to observe when the impurities aggregate; only a relatively broad line in the $g_{\perp}$-region can be observed. Copper impurities were identified in our analysis of these crystals at less than 1 mppm. We were unable to alter the intensity of this line by annealing procedures.

Although it is not clear what, if any, relationship exists between the intensities of the isotropic line and the low-field ODMR line, there are a number of possible interpretations that can be discussed. If the intensities are related, we see at least two distinct possibilities. Assuming the assignment of the low-field line to Cu^{2+} is correct, the strong isotropic line at the position of g_{avg} would result from the hole bound to the copper ion recombining with a near-neighbour, shallowly bound electron. This more diffuse exciton complex has been called an intermediate exciton; a single isotropic line is typically seen at the average of the bound electron and hole's g-values. In the limit where the exchange interaction is small compared with the Zeeman interaction (as in the donor or acceptor resonances), separate lines are detected for each trapped electron and hole species. In the opposite limit, a single resonance is seen at the average of the electron and hole g-value; if the exchange interaction is anisotropic this lines splits, typically into a pair, separated by $2D$ at high fields. This latter case is an appropriate representation for the STE species in AgCl, whereas the former case is an appropriate representation for the STH and the nearly free electron resonances. Intermediate-case excitons are also

characterised by a single line at the average of the electron and hole's g-value; however, because the exchange interaction is smaller than in a 'well-formed' exciton, this line is not split, but merely broadened. The intermediate strength of the exchange interaction results from the fact that the electron and hole do not interact on the same centre, but over short distances, typically over near-neighbour distances. Such intermediate excitons have been identified in II–VI materials (Davies and Nichols 1982, Killoran *et al* 1982, Kana-ah *et al* 1987, Chamel *et al* 1976).

There is an alternative interpretation for the relatively weak and broad ODMR line at 832 mT. Its position is appropriate for the dynamic average of $g_{\parallel}$ and $g_{\perp}$ of the STH. There is then an obvious relationship between the intensities of the lines mentioned above since the STE forms as a result of electron capture at a STH. If this interpretation is correct, both static and dynamically distorting STEs and STHs participate in the AgCl recombination at 4.2 K. It is, then, no longer clear that the addition of the electron to a STH to form the STE lowers the barrier for dynamic distortions since there is evidence for the dynamic effects in the STH before electron capture has occurred. This lowering of the tunnelling barrier was suggested by Yamaga *et al* (1985).

ODMR spectra were recorded at 36 GHz in order to determine what features were present in the spectrum at this higher frequency. Resonances due to the STH and the nearly free electron were clearly identified in agreement with the published spectra. With a [100] orientation of the crystal, a five-line pattern was observed in the centre portion of the spectrum. The g-value of the very strong isotropic line matched the 24 GHz data; the ratio of the intensities for the isotropic line to the remaining four lines (transitions of the D-split STE parallel and perpendicular configurations) was significantly greater than for our 24 GHz experiments. We did not detect the three lines ascribed to a tetragonally distorted electron trapping species, originally assigned by Marchetti and Tinti 1981).

EPR measurements were made on nominally pure single crystals of AgCl at 35 GHz during continuous illumination with 365 nm light. At 1.8 K, signals characteristic of the STH and shallowly trapped electrons were observed as well as a strong single line at $g = 1.975 \pm 0.001$. Refer to figure 7. The signals were detected with a field modulation frequency of 10 kHz; other instrumental factors limit detection to species with lifetimes $\geqslant$10 ms. All of these signals disappeared when the sample was warmed to 4.2 K.

It was suggested in earlier work (Marchetti *et al* 1978) that the observed differences in the species detected by ODMR might be ascribed to the difference between the excitation sources that were employed, that is, to the difference between UV and x-

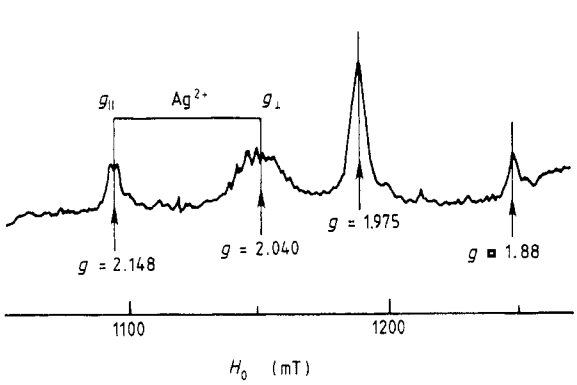

Figure 7. Low-temperature EPR of AgCl. The signal was recorded in dispersion mode. ($\boldsymbol{H}\|[100]$; 35 GHz; $T = 1.8$ K; 365 nm.)

ray excitation. Subsequent work by Yamaga (Yamaga *et al* 1983, Yoshioka and Yamaga 1985, Yoshioka *et al* 1985, Sugimoto *et al* 1985, Yamaga and Yoshioka 1987) and our own efforts have shown that this is not the case. We see essentially no difference in the spectra excited by x-rays and a 313 nm UV source.

We assign the ODMR lines seen at 36 GHz to the same set of defects as observed at 24 GHz for the following reasons. In general, there are a number of experimental conditions that could change the intensities of the observed lines, favouring the observation of the $g = 1.97$ isotropic line, and thus make the identification of the STE transitions difficult. In our 36 GHz ODMR spectrometer, the use of low modulation frequencies is precluded by the noise generated by boiling liquid helium at 4.2 K. This fact alone is sufficient to change the intensity ratio described above. Refer to figure 2, where the change in modulation frequency from 102 to 325 Hz clearly enhances the intensity of the isotropic line. In addition, the model developed by Yamaga for the polarisation selection rules for transitions of the STE (Yoshioka *et al* 1985) suggests that the observation of the STE lines in the Voigt geometry is more difficult than in the Faraday configuration. This is because π-polarised transitions of the STE are observable in the Voigt configuration, but not in the Faraday configuration. Using the spin–lattice relaxation rates derived for this model, such ODMR transitions would be expected to produce intensity *decreases* at resonance. These negative-going lines were, in fact, observed in the case of the Br^- STE by Yamaga and Hayes (1982a) when the Voigt geometry and appropriate polarisers were used to select the π-polarised transitions. When added to the intensity increases at resonance for σ-polarised lines, a near cancellation of the ODMR intensity would result. Finally, it is not yet clear to what extent variations in materials parameters, such as background impurity levels and residual strains, affect the observation of the lines assigned to the various defect species in AgCl. Yamaga's analysis of the exciton ODMR intensities in AgCl requires symmetry breaking either by an odd-symmetry vibrational mode or a nearby impurity. Thus, material factors are expected to play a role in determining relative ODMR line intensities.

The observation of EPR from an excited-state triplet species is quite unusual. Apparently, the extended radiative lifetime for this defect makes this possible. Sugimoto *et al* (1985) estimate the average radiative lifetime for the STE as 2.5 ms; this estimate is entirely consistent with our recording of the signal by EPR. Note that only the $g = 1.975$ lines of the STE was observed. This is in accord with our observations by ODMR that higher modulation frequencies (10 kHz in the EPR experiments) accentuate this resonance relative to the $STE_{\parallel}$ and $STE_{\perp}$ resonances.

4. Conclusions

Although we are not able conclusively to rule out the existence of a tetragonally distorted electron-trapping site in AgCl, its existence seems less likely for the reasons discussed above. Our re-interpretation of these data suggests that exciton effects are certainly evident in the AgCl recombination photophysics at 4.2 K. We believe that the previous assignment of the central features of the 36 GHz ODMR spectrum to a tetragaonally distorted electron trap is incorrect. It is important to emphasise that no single recombination mechanism dominates the photophysics of AgCl; both excitonic and donor–acceptor mechanisms are required to explain the data. We can suggest that both experimental and material factors may enter into determining the relative

intensities of the ODMR lines seen from the self-trapped exciton and the isolated donors and acceptors.

We have extended the measurements of Yamaga and co-workers to include the modulation frequency dependence for the perpendicular transitions of the bromide-associated self-trapped exciton. These data and the results of our wavelength dependences lend support to the assignment of these lines to these same perpendicular configurations of the Br^- STE.

Unlike the Br^- STE, the dynamics of the intrinsic STE in AgCl are not completely understood. We believe that the assignment of the isotropic line at $g = 1.97$ to the dynamic average of the STE transitions is reasonable, even though the different modulation frequency dependence has yet to be explained. Furthermore, we find it attractive to identify the previously unassigned line at $g = 2.09$ with the dynamic average of the STH, although such an assignment must be viewed as tentative.

Because of their relatively high intensity, the transitions of the intrinsic STE, and perhaps the dynamic average of the STE transitions, may be amenable to study by more advanced techniques, such as ODENDOR. In this way, questions about the environment of the STE (impurity- and strain-related effects) can be more fully explored.

Acknowledgments

The analysis of the spectra benefitted from many fruitful discussions with Professor J M Spaeth, University of Paderborn. The authors also wish to acknowledge A P Marchetti (Eastman Kodak Research Laboratories) for his sharing of experimental data and criticism of these ideas.

References

Burberry M S and Marchetti A P 1985 *Phys. Rev.* B **32** 1192
Burnham D C and Moser F 1964 *Phys. Rev.* **136** A744
Chamel M, Chicault R and Merle d'Aubigné Y 1976 *J. Phys. E: Sci. Instrum.* **9** 87
Davies J J and Nichols J E 1982 *J. Phys. C: Solid State Phys.* **15** 5321
Eachus R S, Graves R E and Olm M T 1978 *Phys. Status Solidi* b **88** 705
Hayes W and Owen I B 1978 *Phys. Lett.* **68A** 255
Höhne M and Stasiw M 1968 *Phys. Status Solidi* **28** 247
Kana-ah A, Cavenett B C, Monemar B and Gislason H P 1987 *Semicond. Sci. Technol.* **2** 151
Killoran N, Cavenett B C and Levy F 1982 *Solid State Commun.* **44** 459
Marchetti A P and Burberry M S 1983 *Phys. Rev.* B **28** 2130
—— 1985 *Cryst. Latt. Defects Amorph. Mater.* **12** 329
Marchetti A P, Burberry M S and Spoonhower J P 1988 *Int. Conf. on Defects in Insulating Crystals (Parma, Italy, 1988) Abstracts*
Marchetti A P, Eachus R S and Tinti D S 1978 *Phys. Lett.* **65A** 363
Marchetti A P and Tinti D S 1981 *Phys. Rev.* B **24** 7361
Murayama K, Morigaki K, Sakuragi S and Kanzaki H 1976 *J. Lumin.* **12/13** 309
Sugimoto N, Yoshioka H and Yamaga M 1985 *J. Phys. Soc. Japan* **54** 4331
Yamaga M and Hayes W 1982a *J. Phys. C: Solid State Phys.* **15** L75
—— 1982b *J. Phys. C: Solid State Phys.* **15** L1215
Yamaga M, Sugimoto N and Yoshioka H 1983 *J. Phys. Soc. Japan* **52** 3637
—— 1985 *J. Phys. Soc. Japan* **54** 4340
Yamaga M and Yoshioka H 1987 *J. Phys. C: Solid State Phys.* **20** 2773
Yoshioka H, Sugimoto N and Yamaga M 1985 *J. Phys. Soc. Japan* **54** 3990
Yoshioka H and Yamaga M 1985 *J. Phys. Soc. Japan* **54** 841